

Real-Space Imaging of the Molecular Organization of Naphthalene on Pt(111)

V. M. Hallmark, S. Chiang, J. K. Brown, and Ch. Wöll^(a)

IBM Research Division, Almaden Research Center, San Jose, California 95120

(Received 24 July 1990)

The first application of the scanning tunneling microscope to determine a previously unknown adsorbate orientation is presented for naphthalene adsorbed on Pt(111). Measurements in ultrahigh vacuum explore the details of molecular organization for both ordered and disordered systems and allow tentative assignment of the molecular binding site. Statistical analysis of the molecular packing within close-packed domains is inconsistent with the expected ordered structure for this system. Real-space imaging at submonolayer coverage reveals discrete molecular rotation among allowed orientations and translation between adjacent binding sites at room temperature.

PACS numbers: 68.35.Bs, 61.16.Di, 68.55.Ln

The ability of the scanning tunneling microscope (STM) to produce high-resolution images of molecule/metal systems has been well demonstrated.¹⁻³ Molecular imaging has proven to be possible for those adsorbates which are highly localized, either due to packing constraints or to strong interactions between the molecules and the metal surface. For systems meeting this limitation, STM is on the verge of assuming its eventual role as a routine analytical probe of molecular adsorbate structure. This Letter describes the first application of the STM method to explore adsorbate organization in a system where unresolved questions remain, rather than verification of well-documented proposed structures.

We describe the STM imaging of naphthalene adsorbed onto Pt(111), which allows determination of the absolute molecular orientation, tentative assignment of the adsorbate binding site, and differentiation between ordered and disordered overlayers. Aspects of the molecular interactions which influence packing and domain formation are characterized. We observe novel molecular organization which meets the known low-energy electron-diffraction (LEED) symmetry requirements for this system through pseudo-ordering rather than via the predicted perfect unit-cell structure. This observation has important implications for the utilization of LEED to infer structure in complex molecular systems. We report the first STM detection of molecular rotation among permitted orientations and discrete translation between adjacent binding sites for molecules not confined within close-packed domains. The influence of segregated impurities on both the molecular adsorption and the step formation on the metal substrate is also investigated for the first time.

Previous investigations of naphthalene adsorbed on Pt(111) have revealed the existence of both ordered and disordered overlayer structures.⁴⁻⁶ The disordered structure, resulting from room-temperature exposure to naphthalene vapor, yields only a diffuse, partially segmented $\frac{1}{3}$ -order ring in LEED. The ordered overlayer is achieved either by maintaining the substrate at a tem-

perature between 100 and 200°C during the deposition or by annealing a disordered sample within this temperature range (molecular decomposition occurs above 200°C).⁶ Auger electron spectroscopy (AES) and work-function measurements of the ordered system support the adsorption of the naphthalene molecules with the rings parallel to the metal surface and with the molecular centers separated by three platinum atoms.⁴ This spacing fits well with the van der Waals dimensions for naphthalene,⁴ $8.12 \text{ \AA} \times 7.36 \text{ \AA} \times 3.4 \text{ \AA}$, compared with the platinum near-neighbor distance of 2.77 Å. This overlayer is characterized by a (6×3) LEED pattern, with three equivalent domains of a proposed herringbone unit-cell structure consisting of parallel rows of molecules, with two possible molecular orientations alternating from row to row.⁶ The orientation and registry of the molecules with respect to the metal atoms have not been previously ascertained because of the lack of dynamical LEED analysis for this system. The disordered structure is anticipated to arise from random rotation of these molecular domains with respect to the substrate lattice.⁶

Both ordered and disordered naphthalene/Pt(111) systems were explored using a multichamber ultrahigh-vacuum STM system,⁷ equipped with extensive preparation and analysis facilities. The Pt(111) crystal was subjected to extended oxygen treatment at 10^{-6} torr and 600°C to reduce bulk carbon contamination. Subsequent routine cleaning was achieved by cycles of argon bombardment at 500 eV and annealing to 800°C for 2 min. Naphthalene was admitted to the preparation chamber (base pressure $< 10^{-10}$ torr) from a gas handling line maintained at 75°C. Because of the constraints posed by having a mobile sample, accurate measurements of the substrate temperature during the deposition process were not possible. The ordered overlayer was prepared by annealing the sample to 800°C, allowing the crystal to cool for the minimum time required to prevent molecular decomposition, and then exposing the sample to naphthalene vapor. Successful preparation of the ordered system was judged by the acquisition of

(6×3) LEED patterns comparable to published photographs.⁶ Room-temperature exposures yielded the expected segmented, $\frac{1}{3}$ -order LEED ring, while submonolayer coverage naphthalene preparations (~ 0.2 monolayer) only slightly diminished the intensity of the LEED peaks of clean Pt(111). All STM images were acquired at room temperature in the constant-current topographical mode, with typical collection times of 5–10 min per frame. Positive sample biases near 1 V yielded the highest-quality images. Image processing was limited to low-pass filtering unless otherwise described.

A high-resolution STM image of the ordered naphthalene/Pt(111) system is shown in Fig. 1(a), where the elongated features of individual naphthalene molecules are easily discerned. Internal structure beyond this bilobed character was tip dependent, and attempts at higher-resolution imaging were unsuccessful due to severe imaging instabilities and apparent tip-molecule interactions at low bias voltages or slower scan rates (≤ 15 Å/sec). Superposition of a Pt(111) lattice (with arbitrary location of the molecular centers at on-top sites) reveals that the molecular centers correspond quite well with the expected (3×3) superlattice spacing. Mapping was performed with a group of six molecules, and the fit was judged by the resultant positions of the remaining molecules after the transformation. A schematic of the superposition is shown in Fig. 1(b) for the inscribed region of Fig. 1(a). Molecules belonging to a number of (3×3) domains are easily perceived and the expected herringbone packing is not apparent.

Three distinct equivalent orientations, 120° apart, are

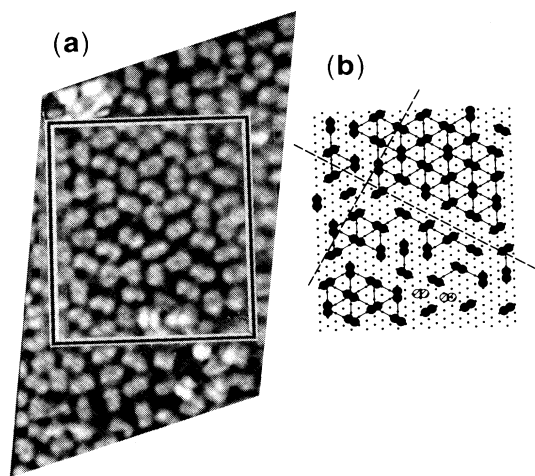


FIG. 1. (a) High-resolution STM image of ordered naphthalene on Pt(111), ~ 90 Å \times 150 Å in size, acquired with a sample bias of $V_s = +0.822$ V and a tunneling current of $I_t = 2.5$ nA. The image skewing is due to the correction for severe thermal drift at the time of data collection. (b) Schematic of the overlay of a Pt(111) lattice with molecular positions. Glide symmetries are indicated by dashed lines.

observed for the naphthalene molecules. Because the (3×3) mapping of the molecular centers reveals the near-neighbor (nn) directions of the substrate lattice, it is possible to assign the absolute orientation of the long naphthalene molecular axis as parallel to the nn direction. Knowledge of the absolute orientation makes it possible to speculate the binding site occupied by naphthalene molecules on the Pt(111) surface. The choice of sites lies between two alternatives with the required *threefold* symmetry: either a hollow site or an on-top site. Placing a naphthalene molecule into a hollow site with the long axis parallel to the nn direction of the platinum lattice breaks the molecular symmetry. The on-top site preserves both molecular and rotational symmetry, as well as providing a coordination number of seven metal atoms, as compared with five for the hollow site. Thus, we tentatively assign the binding site to the on-top site.

Also evident within the image of Fig. 1(a) are several bright features, which have the same bi-lobed structure and lateral dimensions of the naphthalene molecules. These defects appear to the STM to be approximately twice the height of the typical 1-Å naphthalene corrugation. As shown by the hatched molecules in the schematic of Fig. 1(b), the defects correspond quite well to molecules having orientations other than the three standard axial directions, with neighboring molecules located much closer than the allowed (3×3) domain spacing. We conjecture that these defects may correspond to naphthalene molecules tilted on edge.

While the molecular packing within the domains is not the expected herringbone structure, there is a high degree of order. A statistical analysis of the molecular orientations within larger domains, including that in Fig. 1, discloses severe restraints upon the permissible molecular interactions. Considering the long axis of individual molecules within molecular pairs, four *distinct* orientational configurations exist: end-on (*E*), with the molecular axes collinear (—); parallel (*P*), with the axes in the same direction but not collinear (||); normal (*N*), with the axis of one molecule pointing at the center of the other molecule (\perp); and vee shaped (*V*), with the axes separated by 120° and not intersecting within either of the molecules (*V*). There are 3^2 total configurations for a molecular pair and consideration of the degeneracies yields probabilities as follows: $E = \frac{1}{9}$, $P = \frac{2}{9}$, $N = \frac{4}{9}$, and $V = \frac{2}{9}$. The observed frequencies of appearance for these configurations, within (3×3) domains, are $E = 0.0$, $P = 0.18 \pm 0.05$, $N = 0.67 \pm 0.06$, and $V = 0.15 \pm 0.05$ (stated errors are 95%-confidence levels). The end-on configuration is not observed within ordered domains, but often appears at domain boundaries where the molecules are separated by more than three Pt atomic spacings, suggesting a role for this configuration in the formation of the domain walls. The proposed herringbone structure eliminates both the *E* and *V* configurations,

with $E=0.0$, $P=0.33$, $N=0.67$, and $V=0.0$, and is therefore not consistent with the STM observations, where P and V appear with essentially equal probability.

The distinguishing characteristics of the (6×3) LEED pattern which must be accounted for in the observed structure are $\frac{1}{6}$ -order spots and missing beams which indicate glide-plane symmetries within the overlayer.⁸ Although the proposed herringbone structure was motivated by these factors, other structures may satisfy the symmetry requirements. Analysis of the molecular packing within the observed (3×3) domains reveals that $\sim 40\%$ of the molecules conform locally to the required glide-plane symmetry operations. Approximately 30% of the molecules display correlated orientations at 6 times the Pt spacing. Extended sequences of alternating N configurations are present, as they would be in the proposed herringbone structure. These correlations seem sufficiently high to account for the observed LEED pattern, and we conclude that the perfect order of the proposed herringbone packing is not necessary. Location of the molecular centers on a (3×3) superlattice with appropriate correlations of allowed orientational configurations combine to yield molecular organization with pseudo- (6×3) symmetry.

The small size of the pseudo- (6×3) domains, typically containing ≤ 60 molecules, is quite easily discerned in

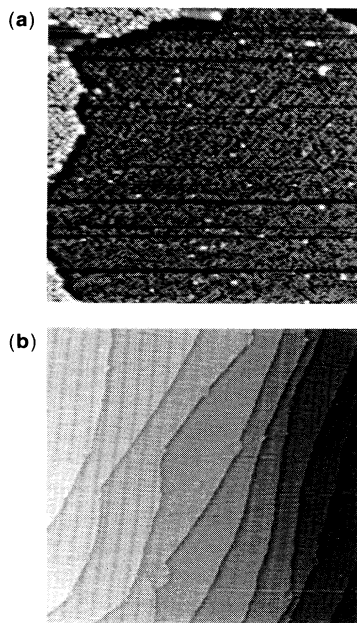


FIG. 2. (a) $400\text{-}\text{\AA}\times 400\text{-}\text{\AA}$ region of an ordered naphthalene/Pt(111) surface. $V_s = +1.012$ V and $I_t = 0.7$ nA. (b) Pt(111) surface without adsorbed naphthalene, showing exceptionally high segregated carbon contamination ($\sim 4\%$) localized at kinks. The image area is $\sim 3000\text{ }\text{\AA}\times 3000\text{ }\text{\AA}$, $V_s = +0.22$ V, and $I_t = 0.2$ nA. Statistical differencing has been used to enhance the viewing of the many terraces (Ref. 9).

larger images such as that of Fig. 2(a), where domain walls are delineated by dark lines. This image also reveals unusual platinum step structures and impurity islands upon which no naphthalene molecules are observed.

A comparative image of the Pt(111) surface prepared without adsorption of molecular naphthalene is presented in Fig. 2(b). Several monatomic height steps are apparent, as are islands of approximately half the platinum step height. The islands are generally localized at transitions between straight, smooth portions of the platinum steps and curved, rough portions of the same steps. The size and number of the islands correlate with the amount of carbon on the Pt(111) surface, as measured by AES and LEED, and the islands are thus assigned as localized carbon contamination. The correlation between carbon-island location and kink formation on the Pt(111) surface is quite strong.¹⁰ This constitutes the first STM visualization of carbon-island formation on Pt(111), although high-resolution AES and field-ion microscopy studies of carbon islands on Pt tips have been reported.^{11,12}

Figure 3 shows an image of the disordered naphthalene overlayer prepared at room temperature. Close examination divulges that the molecular adsorption of this system is quite similar to that of the ordered system, although the disordered overlayer exhibits a vast increase in defect concentration. Molecules located between the defects again display the three equivalent orientations, with (3×3) domain structures smaller than in the ordered system. As molecules tilted on edge may comprise the molecular defects, the distinction between order and disorder in the adsorption of naphthalene may be ascribed to the ability of the system to accommodate adsorption with the rings parallel to the surface via

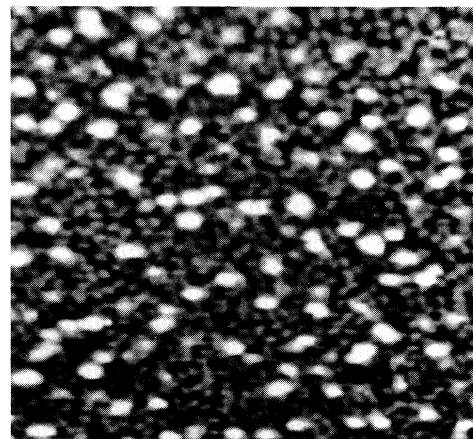


FIG. 3. Image of the disordered naphthalene overlayer. $V_s = +1.53$ V, $I_t = 1$ nA, and the image size is $\sim 300\text{ }\text{\AA}\times 300\text{ }\text{\AA}$.

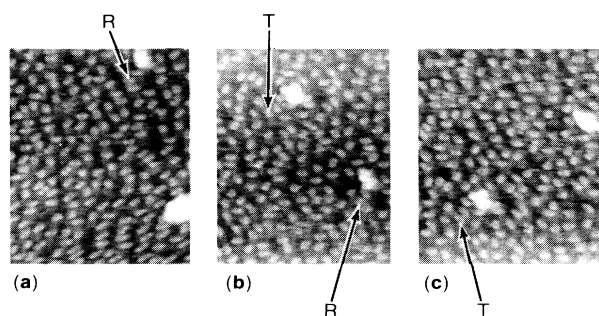


FIG. 4. Sequence of images for the submonolayer naphthalene system, proceeding from (a) to (c), with each image requiring a measurement time of 10 min. Large defects in the images serve as markers to locate specific molecules in sequential images, which exhibit significant drift due to movement of the tunneling tip just prior to the start of the sequence. Molecule *R* undergoes a rotation by $+120^\circ$ between images (a) and (b), while molecule *T* translates by one Pt atom spacing between images (b) and (c). The image size is $\sim 150 \text{ \AA} \times 200 \text{ \AA}$, $V_s = +0.414 \text{ V}$, and $I_t = 0.8 \text{ nA}$.

thermally enhanced motion of the molecules.

Low-coverage adsorption of naphthalene onto Pt(111) exposes the capacity for molecular motion in this system. Careful inspection of the image sequence in Fig. 4 discloses that molecules often undergo discrete rotations among the three equivalent allowed orientations and translations by single Pt lattice spacings. The molecules are uniformly distributed over the Pt surface and no aggregation of molecules occurs, even after several days. Review of the high-coverage, ordered naphthalene system shows limited motion, occurring only at domain boundaries. Within the pseudo- (6×3) domains, rotation of an individual molecule to one of its two alternative orientations would require transition through the forbidden end-on configuration. Simultaneous imaging of molecules and metal corrugation has not been achieved.^{13,14}

In summary, we have made the first STM determination of molecular orientation for naphthalene adsorbed on Pt(111). The three equivalent orientations align the longest molecular axis with the crystallographic directions of the metal surface and favor an on-top binding site. The molecular packing within domains exhibits pseudo- (6×3) ordering rather than perfect unit-cell composition. This aspect of naphthalene adsorption prompts the reconsideration of the symmetry implica-

tions of LEED patterns for systems containing more than one molecule per unit cell and possessing high molecular and substrate symmetry. Disorder in this adsorption system has been shown to result from increased defects, assigned as tilted molecules, and concomitant smaller domains. Discrete molecular rotations and translations among allowed sites are observed at room temperature. Finally, the localization of impurities and determination of the adsorption and kink-formation properties of such impurities by STM imaging should provide insight into the fundamental mechanisms of catalytic processes.

We would like to thank D. J. Coulman, D. DiVincenzo, S. Fain, J. C. Hemminger, C. M. Mate, K. A. R. Mitchell, and M. F. Toney for helpful discussions.

(a)Present address: Angewandte Physikalische Chemie, Universität Heidelberg, Im Neuenheimer Feld 253, D-6900 Heidelberg, Federal Republic of Germany.

¹H. Ohtani, R. J. Wilson, S. Chiang, and C. M. Mate, Phys. Rev. Lett. **60**, 2398 (1988).

²S. Chiang, R. J. Wilson, C. M. Mate, and H. Ohtani, J. Microsc. (Oxford) **152**, 567 (1988); Vacuum **41**, 118 (1990).

³P. H. Lippel, R. J. Wilson, M. D. Miller, Ch. Wöll, and S. Chiang, Phys. Rev. Lett. **62**, 171 (1989).

⁴J. L. Gland and G. A. Somorjai, Surf. Sci. **38**, 157 (1973).

⁵L. E. Firment and G. A. Somorjai, Surf. Sci. **55**, 413 (1976).

⁶D. Dahlgren and J. C. Hemminger, Surf. Sci. **109**, L513 (1981); **114**, 459 (1982).

⁷S. Chiang, R. J. Wilson, Ch. Gerber, and V. M. Hallmark, J. Vac. Sci. Technol. A **6**, 386 (1988).

⁸B. W. Holland and D. P. Woodruff, Surf. Sci. **36**, 488 (1973).

⁹R. J. Wilson and S. Chiang, Phys. Rev. Lett. **59**, 2329 (1987); J. Vac. Sci. Technol. A **6**, 398 (1988).

¹⁰S. Chiang, D. D. Chambliss, V. M. Hallmark, R. J. Wilson, and Ch. Wöll (to be published).

¹¹R. Vanselow and M. Munschau, J. Phys. (Paris), Colloq. **47**, C7-117 (1986).

¹²M. Munschau and R. Vanselow, Surf. Sci. **160**, 23 (1985); J. Phys. (Paris) **47**, C7-121 (1986).

¹³V. M. Hallmark, S. Chiang, J. F. Rabolt, J. D. Swalen, and R. J. Wilson, Phys. Rev. Lett. **59**, 2879 (1987).

¹⁴J. Winttelin, J. Wiechers, H. Brune, T. Gritsch, H. Höfer, and R. J. Behm, Phys. Rev. Lett. **62**, 59 (1989).

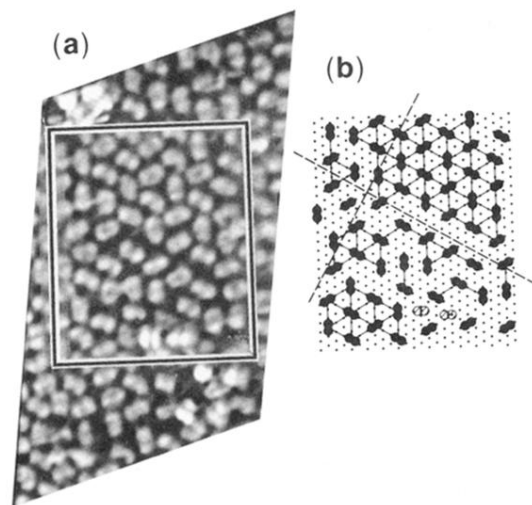


FIG. 1. (a) High-resolution STM image of ordered naphthalene on Pt(111), $\sim 90 \text{ \AA} \times 150 \text{ \AA}$ in size, acquired with a sample bias of $V_s = +0.822 \text{ V}$ and a tunneling current of $I_t = 2.5 \text{ nA}$. The image skewing is due to the correction for severe thermal drift at the time of data collection. (b) Schematic of the overlay of a Pt(111) lattice with molecular positions. Glide symmetries are indicated by dashed lines.

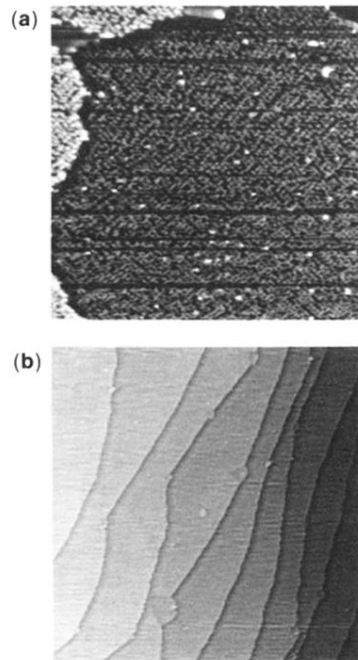


FIG. 2. (a) $400\text{-}\text{\AA} \times 400\text{-}\text{\AA}$ region of an ordered naphthalene/Pt(111) surface. $V_s = +1.012\text{ V}$ and $I_t = 0.7\text{ nA}$. (b) Pt(111) surface without adsorbed naphthalene, showing exceptionally high segregated carbon contamination ($\sim 4\%$) localized at kinks. The image area is $\sim 3000\text{ \AA} \times 3000\text{ \AA}$, $V_s = +0.22\text{ V}$, and $I_t = 0.2\text{ nA}$. Statistical differencing has been used to enhance the viewing of the many terraces (Ref. 9).

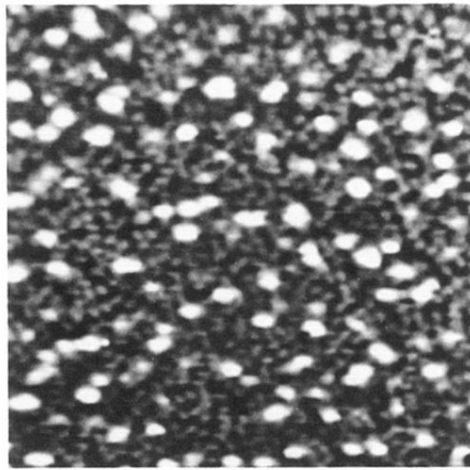


FIG. 3. Image of the disordered naphthalene overlayer. $V_s = +1.53$ V, $I_t = 1$ nA, and the image size is ~ 300 Å \times 300 Å.

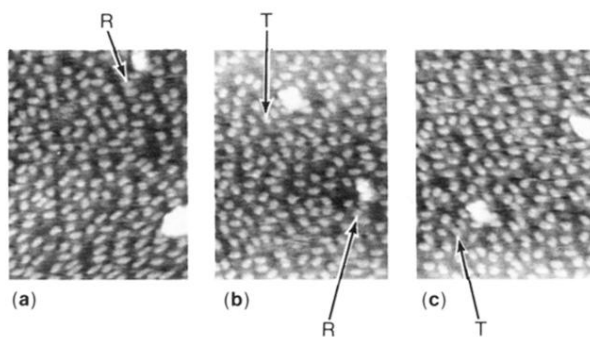


FIG. 4. Sequence of images for the submonolayer naphthalene system, proceeding from (a) to (c), with each image requiring a measurement time of 10 min. Large defects in the images serve as markers to locate specific molecules in sequential images, which exhibit significant drift due to movement of the tunneling tip just prior to the start of the sequence. Molecule *R* undergoes a rotation by $+120^\circ$ between images (a) and (b), while molecule *T* translates by one Pt atom spacing between images (b) and (c). The image size is $\sim 150 \text{ \AA} \times 200 \text{ \AA}$, $V_s = +0.414 \text{ V}$, and $I_t = 0.8 \text{ nA}$.